Local environment perturbations in alpha$_1$-antitrypsin monitored by a ratiometric fluorescent label

Christian Boudier, Andrey S. Klymchenko, Yves Mely and Anny Follenius-Wund*

Received 3rd February 2009, Accepted 20th March 2009
First published as an Advance Article on the web 7th April 2009
DOI: 10.1039/b902309g

The complex multistep inhibition of proteinases by alpha$_1$-antitrypsin (α_1-AT) was investigated by covalently labeling its unique Cys residue with a ratiometric environment-sensitive fluorescent dye, 6-bromomethyl-2-(2-furanyl)-3-hydroxychromone (BMFC). The binding of BMFC-labeled α_1-AT with pancreatic elastase led to significant changes in the dual emission of BMFC. The 8 nm blue shift of one of the bands and *ca.* 65% change in the intensity ratio of the two emission bands suggested an increased exposure of the labeled Cys-232 residue to the bulk water on complex formation. In contrast, the bacterial V8 proteinase-induced cleavage of the reactive center loop of BMFC-labeled α_1-AT did not generate any significant change in the Cys-232 region. Similar experiments with elastase and α_1-AT conjugated to the classical environment-sensitive dye, IANBD, confirmed these results but led to much smaller modifications in the emission spectrum. Stopped-flow investigation of the reaction between BMFC-labeled α_1-AT and elastase showed both a well-described fast and a new slow step of the inhibition process. The latter step is probably associated with the structural reorganization aimed at stabilizing the final complex. These results present a convenient fluorescence ratiometric approach based on the BMFC label for studies of protein conformational changes.

Introduction

The proteins of the "serpin" (SERine Proteinase Inhibitors) superfamily are composed of 350–500 amino acids and share a high homology of structure comprising eight α-helices and three β-sheets. They are widely distributed in higher organisms and plants, as well as in primitive organisms such as viruses. Most serpins are inhibitors of serine proteinases of the chymotrypsin family. As with other inhibitory serpins, alpha$_1$-antitrypsin (α_1-AT) has been shown to irreversibly bind its cognate enzymes through a multistep mechanism.[1–3] The proteinase enzyme recognition site is composed of eight amino acids (referred to as P5-P′3) within the reactive center loop (RCL) of the α_1-AT, an exposed and flexible sequence of ~17 amino acids. First, a reversible Michaelis-type complex forms between the enzyme and the RCL. Proteolysis of the P1-P′1 bond then leads to the formation of a covalent acyl-enzyme intermediate through an ester bond between the serine residue of the enzyme catalytic site and the carbonyl of the inhibitor P1 residue. Cleavage of the exposed RCL triggers a cascade of structural events with the "S(tressed) to R(elaxed)" transition,[4] a large conformational change leading to a much more thermodynamically stable state where the cleaved loop is integrated into β-sheet A. The two X-ray structures of the final inhibitory complex[5,6] show that this insertion pulls the covalently bound proteinase ~70 Å away from the encounter point to the opposite pole of the serpin. In its final position, the enzyme catalytic site adopts a distorted conformation where Ser-195 is moved about 3 Å from its initial position, thus preventing the hydrolysis of the ester bond linking the enzyme and the inhibitor. In this state the inhibitor possesses a higher resistance against guanidinium chloride[7] and thermal denaturation[8,9] than in the native one. Alternatively, the RCL of serpins can be cleaved by numerous proteinases without inhibitory complex formation, in a substrate-like reaction leading to a cleaved and inactive serpin and resulting in the same loop-sheet insertion as that mentioned above.[10,11]

α_1-AT possesses a unique free cysteine residue (position 232) at the C-terminus end of β-strand 1B (Fig. 1).[10] This residue is sufficiently solvent-exposed to bind SH-reactive fluorescent probes as previously shown in FRET experiments aimed at studying the mechanism of complex formation.[12–14] Fluorescent labelling of Cys-232 (and of other engineered Cys residues) with the IANBD probe was also used to investigate the denaturant-induced unfolding of α_1-AT[15] and to probe its structural reorganization following loop insertion and stable inhibitory complex formation.[16] According to this latter study, the S to R transition was found to only poorly affect the environment of Cys-232, in agreement with X-ray data for both the cleaved and complexed states.[5,6]

Labelling of Cys-232 by a more sensitive fluorescent reporter of the environment polarity is an opportunity to further investigate the potential rearrangements of this part of the protein, which is not directly involved in the interaction of the RCL and the β-sheet A or in the proteinase translocation. To this end, we labelled Cys-232 with a new two-colour environment-sensitive fluorescent probe, the 6-bromomethyl-2-(2-furanyl)-3-hydroxychromone (BMFC), recently developed in our laboratory.[18,19] BMFC exhibits excited state intramolecular proton transfer (ESIPT), a reaction yielding a dual emission originating from the normal

Laboratoire de Biophotonique et Pharmacologie, UMR-CNRS 7213, Faculté de Pharmacie, Université de Strasbourg, 74, route du Rhin, 67401, Illkirch-Cedex, France. E-mail: anny.wund@pharma.u-strasbg.fr; Fax: +33(3)90.24.43.12; Tel: +33(3).90.24.42.56

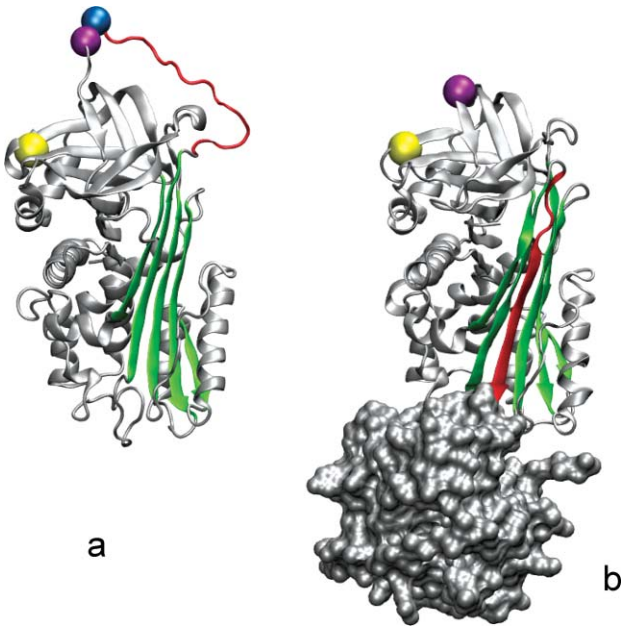

Fig. 1 Three-dimensional representation of human α_1-AT in its free state (a) and complexed with pancreatic elastase (grey surface) (b). In red, the C-terminus side of the reactive center loop becomes part of β-sheet A (green) in the complexed state of the serpin. Cys-232 is represented by a yellow sphere. The P1 and P′1 residues of the reactive center loop are represented by blue and purple spheres, respectively. The figures were prepared with the pdb files 1hp7,[17] and 2d26.[6]

excited form N* and the phototautomer T*, the ESIPT reaction product.[20] These two species account for the well separated (*ca.* 100 nm) short wavelength and long wavelength bands in the emission spectra of 3-hydroxychromones. Importantly, the ESIPT reaction and thus, the ratio of the intensities of the two emission bands in 3-hydroxychromones are strongly dependent on the environment,[21–26] especially on solvent polarity and H-bond donor ability.[25,27] Thus, while in apolar solvents mainly the T* band is observed, in polar protic solvents the N* band is dominant due to H-bonding perturbation of the ESIPT reaction.[22,27–29] Due to the high sensitivity of their dual emission to the environment properties, 3-hydroxychromones are well suited to monitor environment changes at the interfaces of membranes,[30,31] DNA[29] and proteins.[19,32,33] Here, we used BMFC, covalently attached to Cys-232, to probe in the vicinity of the dye, the environmental consequences of the structural changes resulting from the reaction between α_1-AT and either porcine pancreatic elastase (PPE; inhibitory reaction) or bacterial V8 proteinase (substrate reaction). The label was found to exhibit significant changes in its dual emission on the interaction of α_1-AT with elastase. In addition to the classical fast inhibition process, we observe a slow phenomenon on the time scale of 10 min, which indicates the occurrence of slow conformational changes leading to a larger exposure of the labelled Cys to bulk water. In comparison to the classical environment-sensitive label IANBD, the spectroscopic response of BMFC is significantly stronger and ratiometric, which makes it attractive for further applications in protein research.

Experimental

Materials

PPE (EC 3.4.21.36) was purified according to a published procedure.[34] Recombinant α_1-AT expressed in *Escherichia coli* was kindly given as a lyophilized powder by Dr P. Barr (Arriva Pharmaceuticals, USA). V8 proteinase (endoproteinase Glu-C, EC 3.4.21.19) from *Staphylococcus aureus* was from Boehringer (Mannheim, Germany). Succinyl-Ala-Ala-Ala-*p*-nitroanilide (Suc-Ala_3-*p*-NA), the chromogenic substrate of PPE, came from Bachem (Bubendorf, Switzerland). Unless otherwise stated, all reactants and solvents were purchased from Sigma-Aldrich (St Louis, MS). Absolute ethanol and H_2SO_4 were from Merck (Darmstadt, Germany). The chemicals had the highest purity available commercially and were used without further purification. Ultrapure water (Milli Q Instrument, Millipore-Waters Corp., Billerica, MA) was used for the aqueous solutions. All the spectroscopy measurements were carried out in PBS buffer reconstituted from Instamed PBS Dulbecco powder without Ca^{2+}/Mg^{2+} (VWR International, Fontenay-sous-Bois, France) and adjusted to pH 7.1. The α_1-AT concentration was determined by absorption spectroscopy, using $\varepsilon_{280} = 19\,060\ M^{-1}\ cm^{-1}$ for α_1-AT. The enzymatic measurements were carried out at 25 °C in 50 mM Hepes containing 100 mM NaCl (pH 7.4).

Active site titrations

PPE was active site titrated with acetyl-Ala_2-Pro-AzaAla-*p*-nitrophenyl ester (Enzyme System Products). Titrated PPE was used to determine the concentration of active α_1-AT by mixing 22 nM enzyme with increasing concentrations of α_1-AT in 990 µL mixtures. These media were incubated for 45 min to ensure complete enzyme–inhibitor association. The residual enzyme activities were assessed by addition of 10 µL of a 100 mM succinyl-Ala_3-*p*-nitroanilide solution in *N*-methyl pyrrolidone. The concentration of active inhibitor was deduced from the linear inhibition curve. The PPE and α_1-AT concentrations mentioned here refer to active protein concentrations.

Fluorescent probes

BMFC was synthesized in two steps as described earlier[19] using a procedure based on a recently developed methodology.[35] The compound was characterized by ^{1}H-NMR and mass spectroscopy: ^{1}H NMR (300 MHz, $CDCl_3$), 4.60 (2H, singlet), 6.67 (1H, multiplet), 6.94 (1H, singlet), 7.37 (1H, doublet, $J = 5.5$ Hz), 7.55–7.8 (3H, multiplet), 8.24 (1H, doublet, $J = 2.9$ Hz); EI-Mass m/z 320.0 (M^+). IANBD was purchased from Molecular Probes (Eugene, OR). Highly concentrated stock solutions of each fluorescent probe were prepared in DMF at 3.2 mM.

Fluorescent labeling of α_1-AT

The unique Cys residue of α_1-AT at position 232 was labeled with either BMFC or IANBD. Four 25 µL aliquots of BMFC stock solution (2.2 mM in DMF) were sequentially added to 2 mL of 2.7×10^{-5} M α_1-AT solution under continuous stirring. The mixture was allowed to react for 16 h at 4 °C in the dark. The total volume was then applied to a PD-10 gel filtration column

(Amersham Pharmacia Biotech) equilibrated in PBS buffer, pH 7.1 to separate the labeled protein from the free dye. The protein-containing fractions were detected by absorption spectroscopy at 280 nm, pooled and deposited on a second PD-10 column to remove free BMFC adsorbed on the protein.

The same procedure was used for the labeling of α_1-AT by IANBD, although here a 13-fold molar excess of dye was required to obtain a similar degree of labeling.

Determination of the degree of labeling

The extent of label incorporation was determined by absorbance measurements in 1 cm path cuvettes using a Cary IV spectrophotometer (Varian, Australia). The covalently bound BMFC concentration was deduced from the absorbance of the labeled protein sample at 360 nm, assuming that the molar extinction coefficient at 360 nm is the same as that of the free dye in DMF, namely $\varepsilon_{360nm} \sim 16\,400\ M^{-1}\ cm^{-1}$. The absorbance at 280 nm of the sample was used to calculate the α_1-AT concentration after correction for the contribution of BMFC. We found labeling ratios [BMFC]/[α_1-AT] ranging from 0.5 to 0.6. The degree of IANBD labeling was determined in the same way, using $\varepsilon_{478nm} = 25\,000\ M^{-1}\ cm^{-1}$ to obtain the dye concentration.[15] In this case, the labeling ratio [NBD]/[α_1-AT] was 0.4–0.5. The degree of labeling was further checked by titration of the solvent-accessible thiol groups. 6–15 μM of protein were incubated with a 20-fold molar excess of DTNB at room temperature for 10 min. The concentration of free thiol groups (which corresponds to that of the unlabeled protein) was calculated from the absorbance at 412 nm, using a molecular extinction coefficient of $13\,600\ M^{-1}\ cm^{-1}$.[36] By this approach, we found labeling ratios in good agreement with that spectrophotometrically determined. Moreover, active site titration of the BMFC- and IANBD-labeled α_1-AT preparations using PPE (see above) indicated that labeling of Cys-232 did not significantly alter the anti-PPE property of the serpin, in agreement with the literature.[12,16]

Proteolytic inactivation of BMFC-labeled α_1-AT

The labeled α_1-AT (5 μM) was reacted with 0.5 μM of V8 proteinase from *Staphylococcus aureus*.[1] Under these conditions, complete conversion of the intact serpin into its cleaved form was achieved in about 2 min as judged by SDS PAGE (data not shown). To avoid further proteolytic degradation of α_1-AT during the time of the experiments, we did not use higher V8 concentration. Completion of cleavage was also confirmed by checking the disappearance of the anti-PPE property of the treated α_1-AT as described above.

Fluorescence spectroscopy measurements

Steady-state fluorescence spectra were obtained on a Fluoromax spectrofluorometer (Jobin Yvon, USA), with 2 nm excitation and 4 nm emission bandwidths. The fluorescence quantum yields were determined at 20 °C, taking either quinine sulfate in 0.1 M H_2SO_4 ($\phi_{QS} = 0.51$ at this pH)[37] or fluorescein in 0.1 M NaOH ($\phi_F = 0.95$)[38] as a reference. The excitation wavelength was chosen as the best compromise between the absorption band of the compound and that of the reference. At this wavelength, the concentrations were adjusted to an absorbance of 0.1, so that the fluorescence intensities were proportional to the absorbance of the solutions.

Kinetic investigation of the reaction of labeled α_1-AT (5 μM) with the proteinases (5 μM) was performed with a stopped-flow apparatus (SFM-3, Bio-Logic, Claix, France), which allows rapid mixing of 100 μl of each reagent. The fluorescence intensities for the reaction of BMFC-labeled α_1-AT with PPE were simultaneously recorded at 430 nm and above 530 nm (with excitation at 360 nm) using two photomultipliers set at 90° and the appropriate interferential (Melles Griot, France) and cutoff filters (AHF, Germany), respectively. For the reaction of IANBD-labeled α_1-AT with PPE, the fluorescence emission was followed above 530 nm (with excitation at 470 nm). The data recording frequency was $5\ s^{-1}$. Blank experiments in which the enzyme was omitted were performed in the same conditions. Data acquisition and processing were done with the Biokine software from the instrument manufacturer.

Results and discussion

Comparison of the photophysical properties of BMFC and IANBD dyes

We compared the spectroscopic characteristics of BMFC with the well-known environment-sensitive fluorescent dye IANBD in various solvents (Scheme 1, Table 1). Since 3-hydroxychromone dyes show high sensitivity to both polarity and H-bond donor ability of solvents,[25,27,29] we have used the polarity index E^N_T, which accounts for both parameters.[39] The inspection of the data for BMFC shows that the probe is sensitive to this parameter. The absorption maximum presents a small solvatochromism since it red-shifts from 353 to 362 nm with increasing polarity from dioxane to water (Table 1). The fluorescence emission of BMFC is characterized by two bands. The short-wavelength band accounts for the normal excited state species N*, while the long-wavelength band accounts for the excited state tautomer T*. Similar to the absorption maximum, the position of the N* band shifts to the red with increasing solvent polarity. In contrast, the T* band does not correlate with the solvent polarity index E^N_T, but shows a blue shift in protic solvents (Table 1), in line with previous reports on other 3HC derivatives.[27,29] This blue shift is strong in water, *ca.* 30 nm with respect to aprotic solvents; as a consequence, the two bands become closer. Moreover, the ratio of the two emission bands, I_{T^*}/I_{N^*}, also strongly depends on the polarity index E^N_T. An especially dramatic sensitivity of the I_{T^*}/I_{N^*} ratio is observed for polar protic solvents, with a change from 2.2 in ethanol to 0.45 in water. This strong dependence is connected with H-bonding perturbations of ESIPT in protic solvents, resulting in the decrease in the I_{T^*}/I_{N^*} ratio.[25,27,28] Finally, as a general trend, the fluorescence quantum yield decreases when the probe changes from a hydrophobic to a hydrophilic environment, a

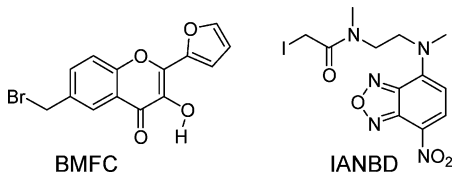

Scheme 1

Table 1 Photophysical characteristics of BMFC and IANBD in various solvents

	BMFC					IANBD		
Solvent[a]	λ_{max}^{abs}/nm	$\lambda_{max}^{em(N^*)}$/nm	$\lambda_{max}^{em(T^*)}$/nm	ϕ^b	I_{T^*}/I_{N^*}[c]	λ_{max}^{abs}/nm	λ_{max}^{em}/nm	ϕ
Dioxane ($E^N_T = 36$)	353	409	538	0.130	9.09	473	523	0.49
Acetone ($E^N_T = 42.2$)	352	412	540	0.063	7.14	480	531	0.069
DMF ($E^N_T = 43.2$)	356	414	541	0.040	7.69	489	538	0.046
EtOH ($E^N_T = 51.9$)	360	420	536	0.064	2.22	478	535	0.112
H_2O ($E^N_T = 63.1$)	362	429	508	0.020	0.45	500	549	0.021

[a] E^N_T is an empirical solvent polarity index.[39] [b] The standard error of the mean for fluorescence quantum yields ϕ is 3% of the value. [c] Average of three different measurements, error is ±0.02.

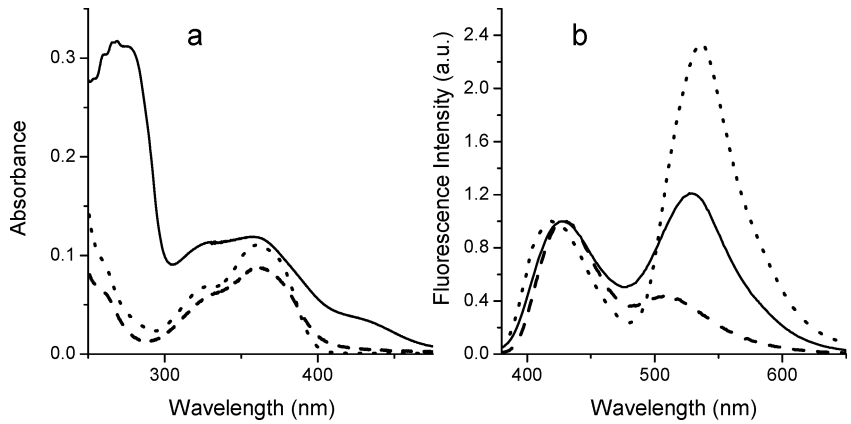

Fig. 2 Steady-state absorption (a) and emission (b) spectra of BMFC in EtOH (···), in H_2O (---) and covalently-bound to α_1-AT (—) in PBS buffer, pH 7.1. The fluorescence spectra were normalized at the N* band maximum. Excitation was at 360 nm.

phenomenon which was also observed with derivatives of the green fluorescent protein chromophore.[40] Similar to the N* band of BMFC, on increasing solvent polarity, IANBD exhibits red shifts of absorption and emission maxima and decreases in its fluorescence quantum yield (except for ethanol). However, in contrast to BMFC, the largest changes in the fluorescence quantum yield of IANBD are observed in apolar media with low E^N_T polarity index ranging between dioxane and acetone. In this respect, BMFC constitutes an environment sensor, more suited for polar media than IANBD. Being attached to biomolecules, BMFC fluorophore should characterize its exposure to bulk water, which can significantly vary upon protein–protein interactions.

α_1-AT has been labelled at its unique and surface-exposed Cys-232 residue. BMFC-labeled α_1-AT shows two main absorption bands with maxima at 269 nm and 360 nm (Fig. 2a). The first, at shorter wavelengths, is characterized by several shoulders corresponding to the absorbance of the two Trp, the six Tyr residues and the twenty-six Phe residues of the protein. The second, due to the absorption of the dye, is close to the band of free BMFC in ethanol, with a maximum at 360 nm. The absence of electrochromic shifts in the covalently labeled BMFC spectrum suggests a selective labeling of the –SH group and a lack of $–NH_2$ groups labeling.[33] Moreover, the excitation spectra (data not shown) are not significantly dependent on the emission wavelength, indicating the absence of ground state (*i.e.* labeling) heterogeneity. The fluorescence emission spectrum of labeled α_1-AT (Fig. 2b) shows well-resolved N* and T* bands, so that band positions and intensities can be determined precisely without additional band separation analysis. One can notice that the bands are nearly of equal width and their positions (N* at 427 nm and T* at 530 nm) are between those of BMFC in ethanol and water (Table 1). The intensity ratio I_{T^*}/I_{N^*} of 1.18 for the labeled protein also fits to the range of ratios observed for BMFC in ethanol and water. These results clearly indicate that the fluorescent probe linked to the protein at its Cys-232 is weakly screened from the bulk water, in line with the surface-exposed position of Cys-232 in the native protein.[16] Moreover, according to the enzymatic titration, BMFC-labeled α_1-AT keeps its full inhibitory activity.

Fig. 3a shows the fluorescence emission spectrum of the free BMFC-labeled α_1-AT and that of its complex with PPE resulting from the reaction of equimolar quantities (10 μM) of enzyme and labeled inhibitor. The complex formation modifies the shape of the fluorescence emission spectrum. The N* and T* bands become closer, as a consequence of a substantial 8 nm blue shift of the T* band and a moderate 2 nm red shift of the N* band (Table 2). Moreover, the binding of elastase to BMFC-labeled α_1-AT also

Table 2 Fluorescence characteristics of labeled α_1-AT in the absence and in the presence of equimolar concentrations of PPE (10 μM)

		λ_{max1}/nm	λ_{max2}/nm	ϕ^a	I_{T^*}/I_{N^*}
BMFC-labeled α_1-AT	–PPE	427	530	0.020	1.18 ± 0.07
	+PPE	429	522	0.014	0.71 ± 0.05
NBD-labeled α_1-AT	–PPE	539		0.030	
	+PPE	540		0.024	

[a] The fluorescence quantum yields represent the mean of at least three different experiments (standard error of the mean = 0.004).

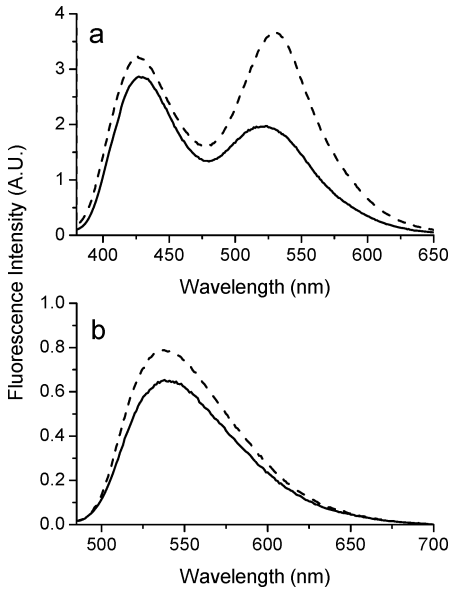

Fig. 3 Steady-state fluorescence emission spectra of 10 μM BMFC-labeled α_1-AT (a) and NBD-labeled α_1-AT (b) in the absence (---) and in the presence (—) of 10 μM elastase in PBS buffer, pH 7.1. Excitation was at 360 nm for BMFC and 470 nm for IANBD.

results in a decrease in the fluorescence intensity and quantum yield, particularly due to the strong drop of the T* band which becomes smaller than the N* band. As a result, the I_{T^*}/I_{N^*} ratio decreases from 1.18 to 0.71. According to the data of BMFC in solvents (Table 1), the observed spectroscopic changes suggest an increase in the water exposure of the label at the Cys-232 site upon interaction of α_1-AT with the enzyme.

α_1-AT was also labeled at Cys-232 with IANBD, an environmentally sensitive fluorescent dye used here as a reference. The fluorescence spectrum shows an emission maximum at 539 nm (Fig. 3b, Table 2), with a 10 nm blue shift and a 43% enhancement of ϕ compared to free IANBD in aqueous buffer (Table 1). Both changes indicate that, similar to BMFC, IANBD reports on a rather high polarity of the site of labeling, in the range between ethanol and water, confirming that the label is only slightly screened from bulk water by neighbor amino acids. The interaction of elastase with NBD-labeled α_1-AT induces a much less perceptible change in the fluorescence spectrum than for BMFC. The emission maximum is not significantly affected by the complex formation (~1 nm red shift) while the fluorescence quantum yield decreases by 20%. These results also suggest an increased exposure of the α_1-AT labeling site to bulk water on α_1-AT interaction with elastase. The much smaller spectroscopic response of IANBD to the inhibitor–enzyme interaction as compared to BMFC can be explained by the significantly lower sensitivity of IANBD in polar environments.

In a previous fluorescence investigation, Ludeman *et al.*[16] reported that almost no conformational change occurs in the region of Cys-232 upon complex formation between NBD-labeled α_1-AT Pittsburgh and thrombin. These authors found no shift of λ_{max}, in agreement with the almost negligible (1 nm) shift observed in our study. However, the small increase in the iodide quenching constant determined by these authors (Stern–Volmer constant $K_{SV} = 9.0\ M^{-1}$ for native α_1-AT and $K_{SV} = 9.7\ M^{-1}$ for the complex) corroborates our results, *i.e.* the exposure enhancement of Cys-232 to bulk water. We also detected a noticeable decrease of the NBD-label quantum yield, a parameter that Ludeman and co-workers did not consider (the spectra presented in their work are normalized). A moderate variation from 0.302 to 0.288 of the quantum yield was also reported by Stratikos and Gettins[14] following the interaction of thrombin with α_1-AT Pittsburgh conjugated to dansyl at Cys-232.

Kinetics of the interaction of labeled α_1-AT with elastase

The reaction of PPE with α_1-AT labeled with BMFC or IANBD was further monitored using stopped-flow mixing and fluorescence detection. The reaction between 5 μM BMFC-labeled α_1-AT and the same concentration of PPE was followed by monitoring simultaneously the fluorescence intensities at 430 nm (I_{N^*}) and above 530 nm (I_{T^*}). The time-dependent traces of the two fluorescence intensities were then used to represent the I_{T^*}/I_{N^*} ratio as a function of time (red trace in Fig. 4a). As expected from the steady state data, this ratio decreases with time, while in a control experiment, where the enzyme was omitted, no changes of the ratiometric response were detected (black trace in Fig. 4a).

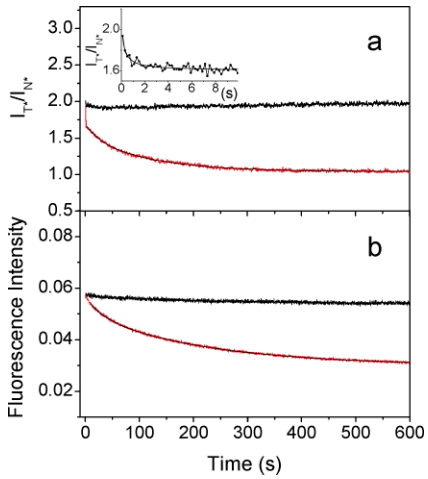

Fig. 4 (a) Kinetics of the interaction of BMFC-labeled α_1-AT with an equimolar concentration of PPE (5 μM). Fluorescence emission was simultaneously monitored at 430 nm and above 530 nm yielding I_{N^*} and I_{T^*}. The I_{T^*}/I_{N^*} ratios for the BMFC-labeled α_1-AT–elastase interaction (red) and for the corresponding blank experiment (black) are represented as a function of time. The first 10 s were fitted to second order kinetics (see inset) whereas the main portion of the curve was fitted to a bi-exponential function. (b) Kinetics of the interaction of NBD-labeled α_1-AT with equimolar concentrations of PPE (5 μM) (red), compared to the corresponding blank experiment (black). Emission was observed at 530 nm. The data were fitted to a bi-exponential function. In (a) and (b), each trace is the average of at least three experiments. The black theoretical curves drawn through the data were generated using the rate constants indicated in Table 3.

Two steps, characterized by very different time-scales, can be recognized. The initial fast decay of the I_{T^*}/I_{N^*} ratio occurs on the time scale of seconds (inset of Fig. 4a). This portion of the signal was best fitted to second order kinetics with a rate constant k_1 of $1.44 \times 10^6\ M^{-1}\ s^{-1}$. Serpins are known to inhibit proteinases by first forming a reversible Michaelis-type intermediate EI* involving the enzyme catalytic site and the inhibitor uncleaved reactive center

Table 3 Kinetics of the α_1-AT–PPE interaction evaluated from stopped-flow measurements

	$k_1/M^{-1}\ s^{-1}$	k_2/s^{-1}	$\alpha_2{}^a$	k_3/s^{-1}	$\alpha_3{}^a$
BMFC-labeled α_1-AT + PPE	$(1.44 \pm 0.3) \times 10^6$	0.040 ± 0.001	0.27 ± 0.01	0.0084 ± 0.0002	0.73 ± 0.01
NBD-labeled α_1-AT + PPE	Not detected	0.042 ± 0.001	0.49 ± 0.01	0.0051 ± 0.0002	0.51 ± 0.01

[a] The amplitudes, α_2 and α_3, were obtained from the bi-exponential fit of the curves shown in Fig. 4.

loop. By stopped-flow fluorescence energy transfer measurements, we previously found a value of 1.5×10^6 M^{-1} s^{-1} for the second order rate constant governing the formation of the intermediate Michaelis complex, under similar experimental conditions.[12] The similarity between the value of this parameter and that of k_1 suggests that the initial fast decay of I_{T^*}/I_{N^*} detected here is likely to be ascribed to structure changes accompanying the Michaelis complex formation. X-Ray data collected from a stable S195A trypsin-serpin Michaelis complex[41] reveal that, besides substantial conformational changes involving the enzyme inhibition site, other structure changes, supposed to unlock the active structure of the serpin were also detected at long distance from the RCL and thus are susceptible to change the probe environment.

This initial transient species was shown to slowly convert into the final stable acyl-enzyme complex EI.[12] The slow decay of the I_{T^*}/I_{N^*} ratio (Fig. 4a) could be satisfactorily fitted to a double exponential model. The best estimates of the first order rate constants k_2 and k_3 were 0.040 ± 0.001 s^{-1} and 0.0084 ± 0.0002 s^{-1}, respectively (see Table 3). Such long-duration conformational changes of a serpin upon its reaction with a proteinase have never been reported so far. Mellet *et al.*[12] found a value of 0.13 s^{-1} for the rate constant governing the conversion of the initial reversible Michaelis complex into a stable species supposed to be the final product of the reaction between PPE and α_1-AT (as measured by FRET), a process involving acyl-enzyme formation and loop insertion with enzyme translocation. Obviously the duration of these events ($t_{\frac{1}{2}} = 5.3$ s) is much shorter than the long-lasting variation of the ratiometric response of BMFC detected in the present study (600 s). The low rate constants found here by kinetic analysis probably describe multiple slow conformational changes of the complex between α_1-AT and the translocated enzyme which occur in the Cys-232 region.

To further investigate the interaction between the two proteins, we monitored the PPE-induced fluorescence intensity changes of IANBD-labeled α_1-AT at 530 nm, in the experimental conditions described above. The time-dependent decrease of the fluorescence intensity upon complex formation is illustrated by the red curve in Fig. 4b whereas the black trace represents the signal resulting from mixing the labeled protein with the buffer. In contrast to BMFC-labeled α_1-AT, the NBD-labeled α_1-AT shows no fast component corresponding to the enzyme inhibition process. However, the data could also be adequately fitted by a double exponential function and the obtained time constants are remarkably close to those measured for the BMFC-labeled α_1-AT–PPE interaction (Table 3).

Thus, while the fast inhibition process could be detected only by the BMFC label, both probes reported on an additional slow process occurring in a time scale much longer than that of α_1-AT–enzyme complex formation. The similar slow kinetic constants obtained with the two probes confirm that the observed process is not a probe-related artifact. It may not be due to an aggregation phenomenon, since the absence at the end of the reaction of aggregated material in the mixture was confirmed by non-denaturing gel electrophoresis (data not shown). In addition, the Rayleigh diffusion peak in the steady-state fluorescence spectra was not broader in the complexed states than in the native states. This indicates that, besides the major structural events accompanying complex formation, more subtle structural modifications alter the side chain conformations in the vicinity of Cys-232 and increase the solvent exposure of the fluorophores. These conformational changes, which have not been described so far, are more than one order of magnitude slower than the disappearance of enzyme activity.

According to crystallographic data,[5,6] the stabilization of the ester linkage that binds the trapped PPE to the serpin in the final complex results from the distortion of the catalytic center of the proteinase. During this step, the proteinase is compressed against the core of the serpin by traction forces resulting from the RCL insertion. It is reasonable to assume that this step, during which the complex is stabilized, likely involves some movements of moderate amplitude that propagate through the serpin architecture up to the β-sheet B where Cys-232 is located. We suggest that a locking of the complex occurs, which prevents the hydrolysis of the acyl-enzyme bond and renders the covalent complex extremely stable.

Interaction of BMFC-labeled α_1-AT with V8 proteinase

We investigated the fluorescence properties of BMFC-labeled α_1-AT reacted with the bacterial V8 proteinase to confirm that the observed slow fluorescence variations are related to the stabilization of the complex and do not accompany the major conformational changes characterizing the S to R transition. This enzyme, which is not a physiological target of α_1-AT, catalytically inactivates the serpin through hydrolysis of the peptide bond between residues Ala and Glu at position P4 and P5 of the RCL, respectively.[1] This triggers a series of conformational changes,[4,42] highly similar to those occurring during the formation of the irreversible α_1-AT–PPE complex. However, opposite to PPE, the insertion into β-sheet A is partial and these conformational changes do not lead to a covalent complex, but to the release of the non-inhibited enzyme. Interestingly, the steady-state fluorescence spectra of intact and V8-cleaved BMFC-labeled α_1-AT (Fig. 5a) are almost identical, indicating that the structural reorganization upon RCL cleavage does not significantly alter the fluorophore environment. The reaction between 5 μM BMFC-labeled α_1-AT and 0.5 μM V8 proteinase was also followed during 600 s after stopped flow mixing of the reagents, a time substantially longer than that required for complete RCL cleavage in these conditions (1.5–2 min as judged by electrophoresis). Fig. 5b shows, with the same scale as in Fig. 4, that no significant change in the I_{T^*}/I_{N^*} ratio of the label is detected. The initial fast decay of the signal observed

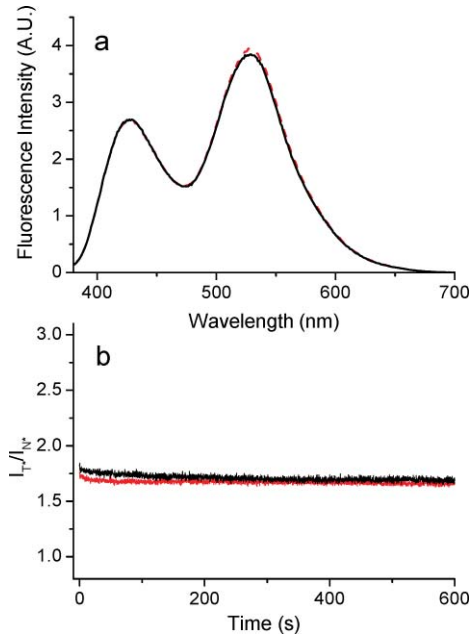

Fig. 5 (a) Fluorescence emission spectra of BMFC-labeled α_1-AT (5 μM) in the absence (black solid curve) and 5 min after the addition (red dashed curve) of V8 proteinase (0.5 μM) in PBS buffer, pH 7.1. (b) Kinetics of the interaction of 5 μM BMFC-labeled α_1-AT with 0.5 μM V8 proteinase. For experimental conditions, see Fig. 4. The I_{T^*}/I_{N^*} ratios for the BMFC-labeled α_1-AT–V8 proteinase interaction (red curve) and for the corresponding blank experiment (black curve) are plotted as a function of time.

for the reaction of PPE with BMFC-labeled α_1-AT was absent, a possible consequence of the low V8 proteinase concentration used. The absence of further fluorescence change of the α_1-AT-BMFC conjugate upon cleavage of the RCL is consistent with the data of Ludeman *et al.*[16] showing that the conformational changes accompanying the papain-induced S to R transformation of α_1-AT labeled at Cys-232 by IANBD also do not modify the fluorescence of the dye. These results clearly evidence the absence of conformational changes in the region of Cys-232 upon the interaction of BMFC-labeled α_1-AT with V8 proteinase and thus suggest that the changes observed with PPE are related to the stabilization of the covalent complex.

The absence of conformational changes during the S to R transition in the Cys-232 vicinity is likely related to the location of Cys-232 on the structurally rigid and highly stable β-sheet B at the rear of the protein.[4,42,43] Since in addition to the major structural changes of the RCL, small rearrangements of the protein core have been shown to accompany the S to R transition,[4] our data suggest that they do not involve the Cys-232 region. However, this region appears to be affected during the stabilization of the covalent acyl-enzyme complex. Nevertheless, the reorganisation of the Cys-232 region is likely local and subtle, as suggested by the close similarity of the structures of the cleaved and complexed forms of α_1-AT.[5,6]

Conclusions

The α_1-AT Cys-232 residue was labeled to better understand the multi-step inhibition of proteinases by serpin by two environment-sensitive dyes: (1) the commonly used IANBD label and (2) a recently developed two-colour dye (BMFC) with strong environment sensitivity for polar media. According to the obtained fluorescence data on both dyes, the interaction of labeled α_1-AT with PPE further exposes the Cys-232 residue to the bulk water. The strong ratiometric response of the BMFC probe allowed us to monitor both the well-characterized fast inhibition reaction (on the time scale of seconds) and a new bi-exponential process that is more than 10-fold slower. Thus, on the first step, the reversible encounter complex between the enzyme and the reactive centre loop of the α_1-AT rapidly converts into a covalent acyl-enzyme intermediate, which on the second step undergoes slow conformational changes. Remarkably, this slow reorganization involves the Cys-232 region, which is involved in a highly rigid region not directly participating to the α_1-AT inhibitory activity. We conclude that consecutive to the formation of the complex at one pole of the serpin, long-range conformational changes occur, which are probably required for further stabilization of the inhibitor–enzyme complex. In addition to the mechanistic insights of the serpin–proteinase interactions never reported so far, the present work proposes the BMFC label as an attractive sensor of fine conformational changes in proteins.

Abbreviations

α_1-AT	α_1-Antitrypsin (α_1-proteinase inhibitor)
PPE	Porcine pancreatic elastase
ESIPT	Excited state intramolecular proton transfer
RCL	Reactive center loop
BMFC	6-Bromomethyl-2-(2-furanyl)-3-hydroxychromone
IANBD	*N*,*N*′-Dimethyl-*N*-(iodoacetyl)-*N*′-(7-nitrobenz-2-oxa-1,3-diazol-4-yl)ethylenediamine
Hepes	4-(2-Hydroxyethyl) piperazine-1-ethane sulfonic acid
DMF	*N*,*N*-Dimethylformamide

Acknowledgements

We acknowledge G. Beauvais and L. Freidja for their experimental help. This work was supported by grants from the Agence Nationale pour la Recherche, the Centre National pour la Recherche Scientifique and the Université de Strasbourg.

References

1 J. Potempa, E. Korzus and J. Travis, The serpin superfamily of proteinase inhibitors: structure, function, and regulation, *J. Biol. Chem.*, 1994, **269**, 15957–15960.
2 W. Bode and R. Huber, Natural protein inhibitors and their interaction with proteinases, *Eur. J. Biochem.*, 1992, **204**, 433–451.
3 P. G. Gettins, Serpin structure, mechanism, and function, *Chem. Rev.*, 2002, **102**, 4751–4804.
4 J. C. Whisstock, S. R. R. W. Carrell and A. Lesk, Conformational changes in serpins: I. The, native and cleaved conformations of alpha1-antitrypsin, *J. Mol. Biol.*, 2000, **295**, 651–665.
5 J. A. Huntington, R. J. Read and R. W. Carrell, Structure of a serpin-protease complex shows inhibition by deformation, *Nature*, 2000, **407**, 923–926.
6 A. Dementiev, J. Dobo and P. G. Gettins, Active site distortion is sufficient for proteinase inhibition by serpins: structure of the covalent complex of alpha1-proteinase inhibitor with porcine pancreatic elastase, *J. Biol. Chem.*, 2006, **281**, 3452–3457.

7 M. Bruch, V. Weiss and J. Engel, Plasma serine proteinase inhibitors (Serpins) exhibit major conformational changes and a large increase in conformational stability upon cleavage at their reactive sites, *J. Biol. Chem.*, 1988, **263**, 16626–16630.

8 K. Katagiri, K. Okada, H. Hattori and M. Yano, Bovine endothelial cell plasminogen activator inhibitor. Purification and heat activation, *Eur. J. Biochem.*, 1988, **176**, 81–87.

9 R. W. Carrell, D. L. Evans and P. E. Stein, Mobile reactive centre of serpins and the control of thrombosis, *Nature*, 1991, **353**, 576–578.

10 H. Loebermann, R. Tokuoka, J. Deisenhofer and R. Huber, Human α_1-Proteinase Inhibitor crystal structure analysis of two crystal modifications, molecular model and preliminary analysis of the implications for function, *J. Mol. Biol.*, 1984, **177**, 531–556.

11 U. Baumann, R. Huber, W. Bode, D. Grosse and M. Lesjak, Crystal structure of cleaved human alpha1-antichymotrypsin at 2.7 A resolution and its comparison with other serpins, *J. Mol. Biol.*, 1991, **218**, 595–606.

12 P. Mellet, C. Boudier, Y. Mely and J. G. Bieth, Stopped flow fluorescence energy transfer measurement of the rate constants describing the reversible formation and the irreversible rearrangement of the elastase-alpha1-proteinase inhibitor complex, *J. Biol. Chem.*, 1998, **273**, 9119–9123.

13 P. Mellet, Y. Mely, L. Hedstrom, M. Cahoon, D. Belorgey, N. Srividya, H. Rubin and J. G. Bieth, Comparative trajectories of active and S195A inactive trypsin upon binding to serpins, *J. Biol. Chem.*, 2002, **277**, 38901–38914.

14 E. Stratikos and P. G. W. Gettins, Major proteinase movement upon stable serpin-proteinase complex formation, *Proc. Natl. Acad. Sci. U. S. A.*, 1997, **94**, 453–458.

15 E. L. James, J. C. Whisstock, M. G. Gore and S. P. Bottomley, Probing the unfolding pathway of alpha1-antitrypsin, *J. Biol. Chem.*, 1999, **274**, 9482–9488.

16 J. P. Ludeman, J. C. Whisstock, P. C. R. Hopkins, B. F. Le Bonniec and S. P. Bottomley, Structure of a serpin-enzyme complex probed by cysteine substitutions and fluorescence spectroscopy, *Biophys. J.*, 2001, **80**, 491–497.

17 S. Kim, J. Woo, E. J. Seo, M. Yu and S. Ryu, A 2.1 A resolution structure of an uncleaved alpha(1)-antitrypsin shows variability of the reactive center and other loops, *J. Mol. Biol.*, 2001, **306**, 109–119.

18 B. E. Cohen, T. B. McAnaney, E. S. Park, Y. N. Jan, S. G. Boxer and L. Y. Jan, Probing protein electrostatics with a synthetic fluorescent amino acid, *Science*, 2002, **296**, 1700–1703.

19 S. V. Avilov, C. Bode, F. G. Tolgyesi, A. S. Klymchenko, J. Fidy and A. P. Demchenko, Temperature effects on alpha-crystallin structure probed by 6-bromomethyl-2-(2-furanyl)-3-hydroxychromone, an environmentally sensitive two-wavelength fluorescent dye covalently attached to the single Cys residue, *Int. J. Biol. Macromol.*, 2005, **36**, 290–298.

20 P. K. Sengupta and M. Kasha, Excited state proton-transfer spectroscopy of 3-hydroxyflavone and quercetin, *Chem. Phys. Lett.*, 1979, **68**, 382–385.

21 P. T. Chou, M. L. Martinez and J. H. Clements, *J. Phys. Chem.*, 1993, **97**, 2618–2622.

22 A. S. Klymchenko and A. P. Demchenko, Multiparametric probing of intermolecular interactions with fluorescent dye exhibiting excited state intramolecular proton transfer, *Phys. Chem. Chem. Phys.*, 2003, **5**, 461–468.

23 S. M. Ormson, R. G. Brown, F. Vollmer and W. Rettig, Switching between charge- and proton-transfer emission in the excited state of a substituted 3-hydroxyflavone, *J. Photochem. Photobiol., A*, 1994, **81**, 65–72.

24 T. C. Swinney and D. F. Kelley, Proton transfer dynamics in substituted 3-hydroxyflavones: Solvent polarization effects, *J. Chem. Phys.*, 1993, **99**, 211–221.

25 A. J. G. Strandjord and P. F. Barbara, The proton-transfer kinetics of 3-hydroxyflavone: solvent effects, *J. Phys. Chem.*, 1985, **89**, 2355–2361.

26 D. McMorrow and M. Kasha, Intramolecular excited-state proton transfer in 3-hydroxyflavone. Hydrogen-bonding solvent perturbations, *J. Phys. Chem.*, 1984, **88**, 2235–2243.

27 A. S. Klymchenko, C. Kenfack, G. Duportail and Y. Mély, Effects of polar protic solvents on dual emissions of 3-hydroxychromones, *J. Chem. Sci.*, 2007, **119**, 83–89.

28 D. McMorrow and M. Kasha, *J. Phys. Chem.*, 1984, **88**, 2235–2243.

29 A. S. Klymchenko, V. V. Shvadchak, D. A. Yushchenko, N. Jain and Y. Mely, Excited-state intramolecular proton transfer distinguishes microenvironments in single- and double-stranded DNA, *J. Phys. Chem. B*, 2008, **112**, 12050–12055.

30 G. M'Baye, Y. Mely, G. Duportail and A. S. Klymchenko, Liquid ordered and gel phases of lipid bilayers: Fluorescent probes reveal close fluidity but different hydration, *Biophys. J.*, 2008, **95**, 1217–1225.

31 V. V. Shynkar, A. S. Klymchenko, C. Kunzelmann, G. Duportail, C. D. Muller, A. P. Demchenko, J. M. Freyssinet and Y. Mely, Fluorescent biomembrane probe for ratiometric detection of apoptosis, *J. Am. Chem. Soc.*, 2007, **129**, 2187–2193.

32 K. Enander, L. Choulier, A. L. Olsson, D. A. Yushchenko, D. Kanmert, A. S. Klymchenko, A. P. Demchenko, Y. Mely and D. Altschuh, A peptide-based, ratiometric biosensor construct for direct fluorescence detection of a protein analyte, *Bioconjugate Chem.*, 2008, **19**, 1864–1870.

33 A. S. Klymchenko, S. V. Avilov and A. P. Demchenko, Resolution of Cys and Lys labeling of alpha-crystallin with site-sensitive fluorescent 3-hydroxyflavone dye, *Anal. Biochem.*, 2004, **329**, 43–57.

34 D. M. Shotton, in *Elastase*, Perlmann and Lorand, New York, 1970.

35 A. S. Klymchenko, G. Duportail, T. Ozturk, V. G. Pivovarenko, Y. Mely and A. P. Demchenko, Novel two-band ratiometric fluorescence probes with different location and orientation in phospholipid membranes, *Chem. Biol.*, 2002, **9**, 1199–1208.

36 G. L. Ellman, Tissue sulfhydryl groups, *Arch. Biochem. Biophys.*, 1959, **82**, 70–77.

37 R. A. Velapoldi and K. D. Mielenz, Standard Reference Materials: A fluorescence standard reference material: quinine sulfate dihydrate, *NBS Spec. Publ. (U. S.) 260-64*, National Bureau of Standards, Washington, DC, 1980, pp. 25–32.

38 J. H. Brannon and D. Magde, Absolute quantum yield determination by thermal blooming fluorescein, *J. Phys. Chem.*, 1978, **82**, 705–709.

39 C. Reichardt, Solvatochromic dyes as Solvent Polarity Indicators, *Chem. Rev.*, 1994, **94**, 2319–2358.

40 A. Follenius-Wund, M. Bourotte, M. Schmitt, F. Iyice, H. Lami, J. J. Bourguignon, J. Haiech and C. Pigault, Fluorescent derivatives of the GFP chromophore give a new insight into the GFP fluorescence process, *Biophys. J.*, 2003, **85**, 1839–1850.

41 S. Ye, A. L. Cech, R. Belmares, R. C. Bergstrom, Y. Tong, D. R. Corey, M. R. Kanost and E. J. Goldsmith, The structure of a Michaelis serpin-protease complex, *Nat. Struct. Biol.*, 2001, **8**, 979–983.

42 P. E. Stein and C. Chothia, Serpin tertiary stucture transformation, *J. Mol. Biol.*, 1991, **221**, 615–621.

43 D. J. Tew and S. P. Bottomley, Probing the equilibrium denaturation of the serpin alpha(1)-antitrypsin with single tryptophan mutants; evidence for structure in the urea unfolded state, *J. Mol. Biol.*, 2001, **313**, 1161–1169.